國 立 交 通 大 學

電子工程學系 電子研究所碩士班

碩 士 論 文

多層架構的鄰近單元交換方法之大型電路佈局

Large-Scale Circuit Placement with Refined Neighborhood Exchange in Multilevel Framework

研 究 生:王冠中

指導教授:陳宏明 博士

中 華 民 國 九 十 四 年 六 月

多層架構的鄰近單元交換方法之大型電路佈局

Large-Scale Circuit Placement with Refined Neighborhood Exchange in Multilevel Framework

研究生：王冠中　　Student：Kuan-Chung Wang

指導教授：陳宏明 博士　　Advisor：Prof. Hung-Ming Chen

國立交通大學

電子工程學系 電子研究所碩士班

碩士論文

A Thesis
Submitted to Department of Electronics Engineering & Institute of Electronics
College of Electrical Engineering and Computer Science
National Chiao Tung University
in Partial Fulfillment of Requirements
for the Degree of
Master of Science
in
Electronics Engineering
June 2005
Hsinchu, Taiwan, Republic of China

中華民國九十四年六月

多層架構的鄰近單元交換方法之大型電路佈局

研究生:王冠中　　　　　　　　教授:陳宏明 博士

國立交通大學　電子工程學系　電子研究所　碩士班

摘　　　要

隨著奈米製程的演進，現今的電路佈局技術將面臨更多的挑戰，例如：大量的不同尺寸的單元佈局、繞線複雜度、延遲、雜訊等。目前晶片設計市場的競爭日益激烈，大家都希望能用更短的時間，更小的面積，更簡易的繞線作出產品。因此現今的單晶片系統設計將需要更快速且更有效的大型積體電路佈局方法。我們將鄰近單元的交換方法應用到多層架構的二元樹電路佈局演算法當中，與過去的演算法相比，能夠在更短的時間內得到更好的佈局結果。

Large-Scale Circuit Placement with Refined Neighborhood Exchange in Multilevel Framework

Student：Kuan-Chung Wang　　　　　　　　Advisor：Prof. Hung-Ming Chen

Department of Electronics Engineering
& Institute of Electronics
National Chiao Tung University

Abstract

In nanometer IC technologies and SoC (System on Chip) design flow, existing placement approaches face many serious challenges, including large size(billions of transistors), mix-size cell placement, wire congestion, and more complex design constraints (delay, noise, manufacturability, etc.). Since the IC design market is more and more competitive, it is necessary to have faster time to market, smaller silicon area utilization, and less wire length for layout. Efficient and effective design methodologies of large scale design placement are essential for modern SoC designs. We improve the ε-neighborhood and λ-exchange to fit in the large-scale circuit placement and use it in the refinement stage of the MB*-tree algorithm to gain a better solution efficiently.

誌謝

首先要感謝的是我的指導教授陳宏明博士，老師不僅在專業上給予學生指導，連生活上的小細節都很關心學生，非常感謝兩年來老師的包容與鼓勵。

另外要感謝實驗室的同學們不吝於幫忙我解決課業上及論文的問題，還有學弟們讓實驗室裡時時充滿歡樂輕鬆的氣氛。

也感謝慧文讓我的研究所生活很充實，吃飯的時候不會覺得無聊，最後要感謝我的家人，讓我衣食無缺的順利完成我的碩士學位。

Contents

1 Introduction **1**

1.1 Organization of this Thesis 2

2 Large-Scale Circuit Placement with Neighborhood Exchange **3**

2.1 B*-tree Representation 3

2.2 MB*-tree 5

2.3 Performance-Driven Module Perturbation 5

2.3.1 Unidirectional Circulation Form 5

2.3.2 Permutation Form 9

2.4 Problem Formulation 12

3 The MBNE Algorithm **13**

3.1 The Clustering Phase 13

3.2 The Declustering Phase 15

3.3 Our Refinement Method In Declustering Phase 18

3.3.1 Null Module Insertion For Further Movement 19

3.4 Floorplanner Flow 20

4 Experimental Results **23**

4.1 *Industry* with MB*-tree (Area, Wirelength, Area/Wirelength) 23
4.2 MCNC - ami49_1-200 with MB*-tree (Area) 24
4.3 GSRC - n100-300 with MB*-tree (Area, Wirelength) 24
4.4 Efficiency with MB*-tree 25

5 Conclusion and Future Works **27**

Bibliography **27**

List of Figures

2.1 An admissible placement and its corresponding B*-tree. 4

2.2 The search tree of unidirectional circulation form, and each node represents a module and each edge represents a trial transformation. . . 7

2.3 Trial interchange of modules, $A{\rightarrow}B{\rightarrow}E{\rightarrow}O{\rightarrow}A$ (λ=4). 8

2.4 Trial interchange of modules, $A{\rightarrow}B{\rightarrow}A$ (λ=2). 8

2.5 Trial interchange of modules, $A{\rightarrow}B{\rightarrow}E{\rightarrow}A$ (λ=3). 9

2.6 A's 1-neighbors $\{B, C, D, E, F\}$ and D's 1-neighbors $\{G, H, I, J, K\}$. 10

2.7 Search tree from A. 10

3.1 The MBNE algorithm flow. Clustering followed by declustering and using our refinement approaches in declustering phase to improve the packing results. 14

3.2 The relation of two modules and their clustering.[10] (a) Two candidate modules m_i and m_j. (b) The clustering and the corresponding B*-subtree for the case where m_i is horizontally related to m_j. (c) The clustering and the corresponding B*-subtree for the case where m_i is vertically related to m_j. 16

3.3 The declustering algorithm.[10] 17

3.4 The definition of ϵ-neighborhood in our refinement method. 18

3.5 An example of λ-exchange, λ=4. 19

3.6 An example of null module insertion for refinement. (a)Insert modele N to replace modele B for swaping. (b)After swap, $A \rightarrow D \rightarrow C \rightarrow N \rightarrow A$. (c)Delete module N. 20

3.7 An example of MBNE algorithm.[10] 22

List of Tables

4.1 Comparisons for area optimization alone, wirelength optimization alone, and simultaneous area and wirelength optimization between MBNE and MB*-tree based on the circuit *industry*. 24

4.2 Comparisons for area, dead space, and runtime between MBNE and MB*-tree with the MCNC benchmark. 25

4.3 The number of modules, number of nets, and total area of the GSRC benchmark. 26

4.4 Comparisons for area and wirelength optimization between MBNE and MB*-tree with the GSRC benchmark. 26

4.5 Comparisons for efficiency between MBNE and MB*-tree with four benchmark. 26

Chapter 1

Introduction

Modern system designs become more and more complex due to the progress of VLSI manufacturing technologies. In nanometer IC technologies and SoC (System on Chip) design flow, existing placement approaches face many serious challenges, including large size(billions of transistors), mix-size cell placement, wire congestion, and more complex design constraints (delay, noise, manufacturability, etc.). Since the IC design market is more and more competitive, it is necessary to have faster time to market, smaller silicon area utilization, and less wire length for layout. Efficient and effective design methodologies of large scale design placement are essential for modern SoC designs.

Many placement methods have been presented in the literature[1,2,3,4,5,6,7,8,9]. However, because of inflexibility in representing non-slicing placement and non-hierarchical data structures, the performance of traditional placement algorithms was not very good. Until recently, the B*-tree representation[1] provided an efficient, effective, and flexible data structure for non-slicing placement. Further, the MB*-tree algorithm[10] has shown a hierarchical and divide-and-conquer framework which is more facilitating to solve placement problem.

On the other hand, the ϵ-neighborhood and λ-exchange algorithm, first presented in [11], was used for standard cell based placement. This method, for permuting cells with wire length driven approach, gave better performance compared with randomly interchanges of cells. This limited trial permutation enable us to find a good local optimum solution more efficient.

In this thesis, we transform the ϵ-neighborhood and λ-exchange to fit in the large-scale circuit placement and use it in the refinement stage of the MB*-tree algorithm. This method searches the solutions in the whole permutation of the selected cells. Although our method ϵ-neighborhood and λ-exchange takes much time for one perturbation (since it needs to search in all permutations), its efficiency will compensate for the computation time by comparing with randomly interchanges.

1.1 Organization of this Thesis

The remainder of this thesis is organized as follows. Chapter 2 gives a brief overview on the B*-tree representation, describes the history of ϵ-neighborhood and λ-exchange refinement method, and formulates the large-scale circuit floorplanning/placement problem. Chapter 3 presents our two-stage algorithm, clustering followed by declustering, also shows a refinement method, and some heuristic methods. Chapter 4 shows the experimental results. Chapter 5 presents the conclusion and future works.

Chapter 2

Large-Scale Circuit Placement with Neighborhood Exchange

There were already many approach to solve the large-scale circuit floorplan/placement issue years ago. For example, in floorplanning, there was MB*-tree[10] which extended from B*-tree[1]; in placement such as MPL[12].

2.1 B*-tree Representation

Given a compacted placement P that can neither move down nor move left called an *admissible placement*, we can represent it by a unique B*- tree T[1]. (See Figure 2.1(b) for the B*-tree representing the placement of Figure 2.1(a).) A B*-tree is an ordered binary tree whose root corresponds to the module on the bottom-left corner. Using the depth-first search (DFS) procedure, the B*- tree T for an admissible placement P can be constructed in a recursive fashion. Starting from the root, we first recursively construct the left subtree and then the right subtree. Let R_i denote the set of modules located on the right-hand side and adjacent to m_i. The left child of the node n_i corresponds to the lowest module in R_i that is unvisited. The right child of n_i represents the lowest module located above m_i, with its x-coordinate equal to that of m_i.

The B*-tree keeps the geometric relationship between two modules as follows. If

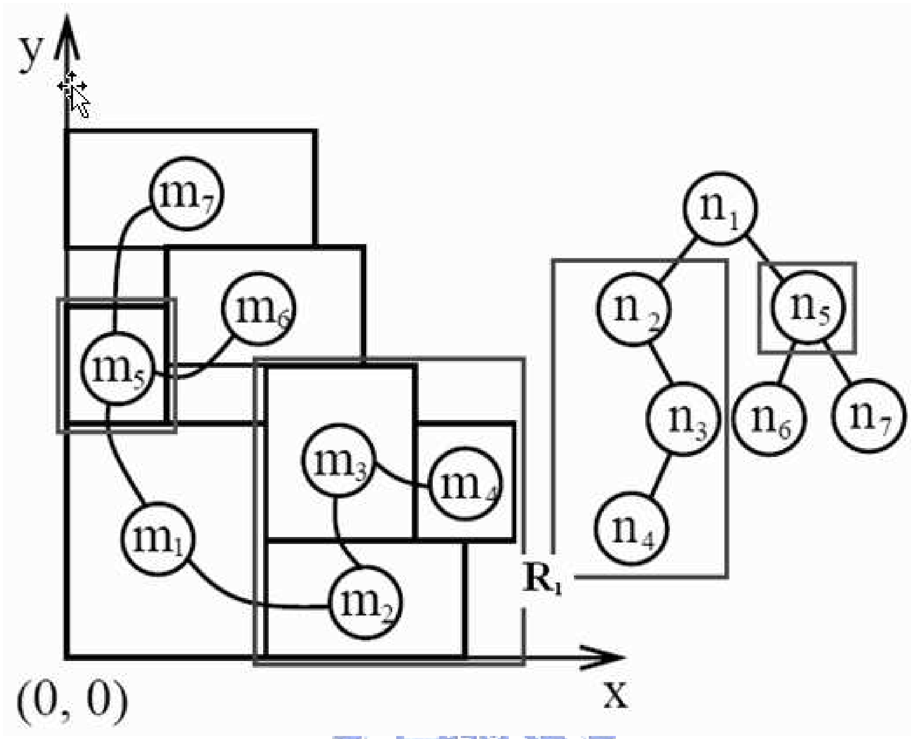

Figure 2.1: An admissible placement and its corresponding B*-tree.

node n_j is the left child of node n_i, module m_j must be located on the right-hand side of m_i, with $x_j = x_i + w_i$. Besides, if node n_j is the right child of n_i, module m_j must be located above module m_i, with the x-coordinate of m_j equal to that of m_i; i.e., $x_j = x_i$. Also, since the root of T represents the bottom-left module, the coordinate of the module is $(x_{root}, y_{root}) = (0, 0)$.

Inheriting from the nice properties of ordered binary trees, the B*-tree is simple, efficient, effective, and flexible for handling non-slicing floorplans. It is particularly suitable for representing a non-slicing floorplan with various types of modules and for creating or incrementally updating a floorplan. What is more important, its binary-tree based structure directly corresponds to the framework of a hierarchical scheme, which makes it a superior data structure for multilevel large-scale building module floorplanning/placement.

2.2 MB*-tree

In [10], a multilevel floorplanning/placement framework based on the B*-tree representation, called MB*-tree, is presented to handle the floorplanning and packing for large-scale building modules. The MB*-tree adopts a two-stage technique, clustering followed by declustering. The clustering stage iteratively groups a set of modules based on a cost metric guided by area utilization and module connectivity, and at the same time establishes the geometric relations for the newly clustered modules by constructing a corresponding B*-tree for them. The declustering stage iteratively ungroups a set of the previously clustered modules (i.e., perform tree expansion) and then refines the floorplanning/placement solution by using a simulated annealing scheme. In particular, the MB*-tree preserves the geometric relations among modules during declustering, which makes the MB*-tree an ideal data structure for the multilevel floorplanning/placement framework.

2.3 Performance-Driven Module Perturbation

Those approaches were first bring forth in [11], and promoted in [12]. But they are all about gate array based placement. We first review those approaches in this subsection, then later show our improvement in our framework for efficient large-scale circuit placement.

2.3.1 Unidirectional Circulation Form

Let us consider a board on which every module is placed. Pick one module, denote it by M. Move only module M on the board, while the other modules remain fixed. The wirelength of a signal net does not change, as long as the signal net is not connected to module M. Therefore, we only need to consider the signal nets connected to module M and the sum of the wirelength of these signal nets. This value is referred to as the wirelength associated with module M.

We now define the *median of module M*. Module M may be placed on $m \times n$ different positions (like Figure 2.3). The median of module M is defined as a position where the routing length associated with module M is minimum. Next, sort all the wirelengths associated with module M with respect to the module M position in ascending order. In this order, choose ϵ elements from the minimum one. The set of these ϵ positions is defined as the *ϵ-neighborhood for median of module M*.

Let S be the set of all feasible solutions of this placement and let x be a feasible solution, $x \in S$. Consider the neighborhood of x, denoted by *X(x)*, which is a subset of S. In the first step, x is set to a feasible solution and a search is made in *X(x)* for a better solution *x'* to replace x. This process, which is referred to hereafter as a local transformation, is repeated until no such *x'* can be found. A solution *x"* is said to be a local optimum if *x"* is better than any other elements of *X(x)*.

Many definitions may be considered for the neighborhood of a solution. The set of solutions transformable from x by exchanging not more than λ elements is regarded as the neighboorhood of x. A solution x is said to be λ-optimum if x is better than any other solutions in the neighborhood in this sense. Although the λ-optimum solution gets better as λ increases, the computation time can easily go beyond the acceptable limit when an exhaustive search is performed for large λ. Therefor we present the following method which does not examine all the elements in the neighborhood, nor does it guarantee a λ-optimum solution. However, it is very efficient in the sense that it can be applied for a large value of λ with limited searches in the neighborhood.

The search procedure is illustrated along with the search tree shown in Figure 2.2, where each node represents a module and each edge represents a trial transformation. The root node of the tree A is a module chosen to initiate the trial interchange, which is referred to as the primary module. A path connecting node A and one of the other nodes defines a possible interchange. For example, the path $A \rightarrow B \rightarrow E \rightarrow O$ refers to the trial interchange of four modules, as shown in Figure 2.3. Here, module A is placed on the slot of B, B is placed on E, E on O, and O on A, in a round robin sequence. Although this transformation is a quadruple interchange, it includes a pairwise interchange as a special case, i.e., paths $A \rightarrow B$, $A \rightarrow C$, and $A \rightarrow D$, as shown in Figure 2.4. Value λ indicates the number of modules to be interchanged.

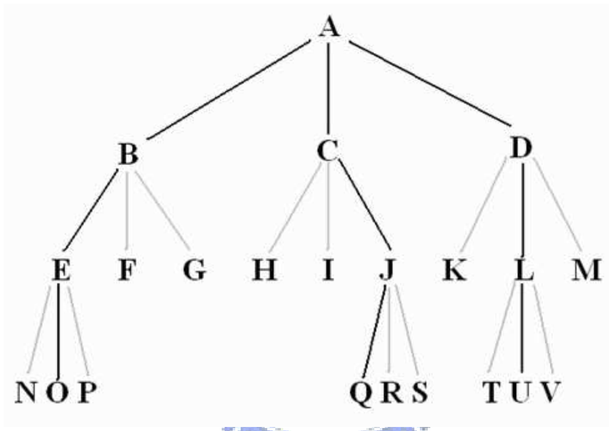

Figure 2.2: The search tree of unidirectional circulation form, and each node represents a module and each edge represents a trial transformation.

The search tree is examined as follows. In this example, ϵ is fixed as 3. First, module A is interchanged with either one of the modules on trial in the ϵ-neighborhood of A median ($\lambda = 2$). The ϵ-neighborhood modules are B, C, and D, thus pairwise interchanges between A and B, A and C, and A and D are performed (Figure 2.4). The trial interchange is accepted if it results in the reduction on the total wirelength. If more than one reduction occurs in these transformations, the interchange with the greatest reduction is selected for acceptance. If no interchange contributes to reducing the total routing length, the next step ($\lambda = 3$)is initiated.

Module A is placed on the slot of B, Then the median of B and its ϵ-neighborhood are calculated. In this case, the ϵ-neighborhood module are E, F, and G. Thus

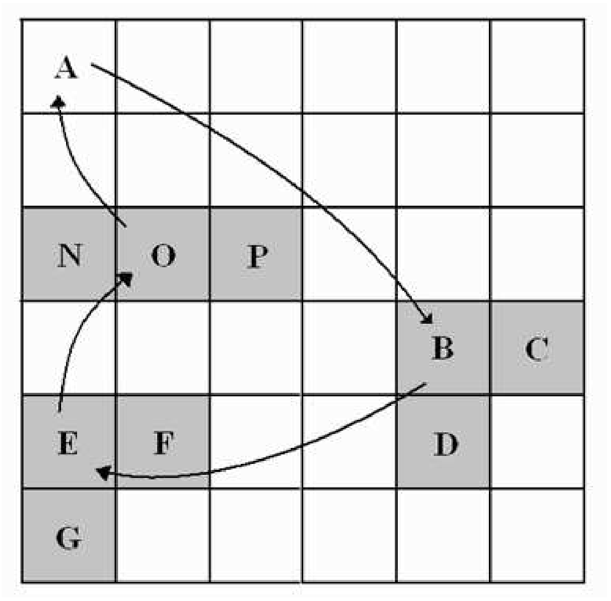

Figure 2.3: Trial interchange of modules, $A \rightarrow B \rightarrow E \rightarrow O \rightarrow A$ (λ=4).

interchanges $A \rightarrow B \rightarrow E$, $A \rightarrow B \rightarrow F$, and $A \rightarrow B \rightarrow G$ are tried, as shown in Figure 2.5.

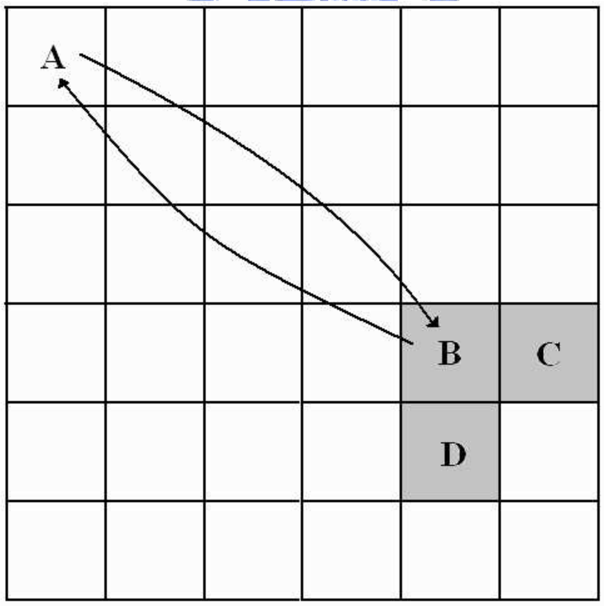

Figure 2.4: Trial interchange of modules, $A \rightarrow B \rightarrow A$ (λ=2).

These trial interchanges are accepted if one of them results in the reduction on the total routing length. Otherwise, we consider the three interchanges of paths

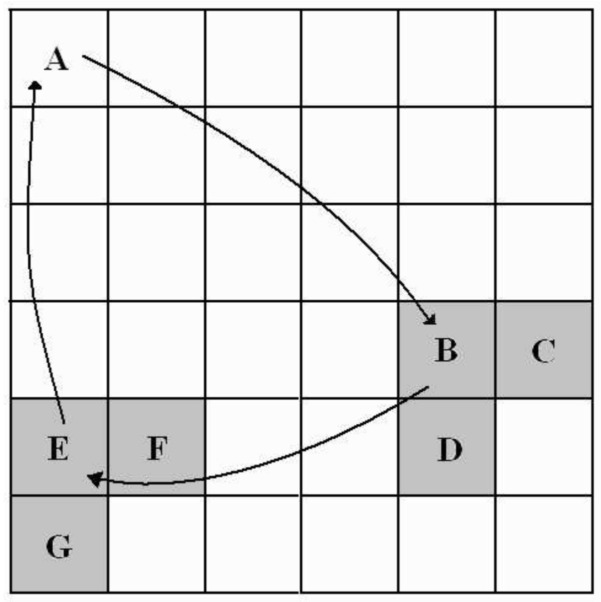

Figure 2.5: Trial interchange of modules, $A \to B \to E \to A$ (λ=3).

$A \to B \to E$, $A \to B \to F$, and $A \to B \to G$, and choose the best one (least total wirelength) for the later tree search. In Figure 2.5, $A \to B \to E$ is chosen.

The solid lines in the tree search shown in Figure 2.2 indicate which searches are to be continued. Broken lines show the searches which are to be terminated. Therefore, no more search efforts are made along paths $A \to B \to F$ and $A \to B \to G$. There is only one solid line under any node, except for root node A. Triple interchanges are performed for the other ϵ-neighborhood modules, C and D, of root node A. Tree search will be continued following J or L, whereas no search will be accomplished through H, I, K, and M. The tree search is continued, i.e., a path from node A is extended as long as λ is no greater than λ*, which is given as a parameter.

2.3.2 Permutation Form

This algorithm is based on the concepts from previous form. Assuming all modules except v are fixed in their current locations, we can compute v's optimal slot locations. Suppose v's optimal slot location is *(r,c)* where r is the row index and c is column index in our grid. Modules located in slots at *(i,j)*, where $|i\text{-}r|+|j\text{-}c| \leqq \epsilon$, are called ϵ-neighbors of module v. For instance, in Figure 2.6, suppose the optimal slot location of module A is occupied by module B. A's 1-neighbors ($\epsilon = 1$) are $\{B, C, D, E, F\}$. Similarly, assuming that D's optimal slot is taken by G, we say module D's 1-neighbors are $\{G, H, I, J, K\}$.

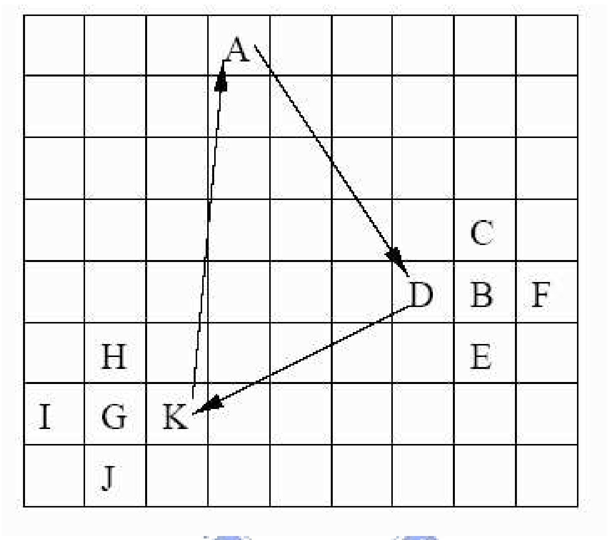

Figure 2.6: A's 1-neighbors $\{B, C, D, E, F\}$ and D's 1-neighbors $\{G, H, I, J, K\}$.

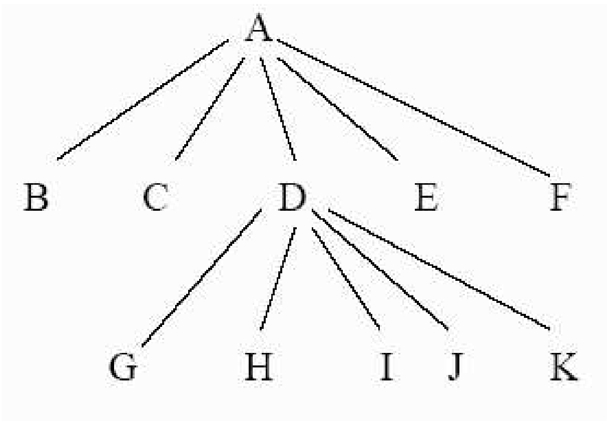

Figure 2.7: Search tree from A.

This algorithm uses a different λ-exchange algorithm from previous form. In unidirectional circulation form, starting from a module v_1, we compute all of its

ϵ-neighbors. This procedure generates a search tree, each leaf defines a module-exchange sequence. We use part of the search tree from module A as example, as shown in Figure 2.7. With ϵ=1 and λ=3, we use the following exchange sequence for leaf K: $A \rightarrow D \rightarrow K \rightarrow A$, i.e., move module A to D's slot, move D to K's slot, and move K to A's slot. The best module exchange sequence will be chosen, or no exchange is made when the original placement has a smaller cost. This method has two major drawbacks. First, the size of the search tree grows very quickly with slight increase of ϵ and λ. Second, the module exchange sequence may not be the best possible. Intuitively, moving a module into its ϵ-neighborhood has a high probability of reducing the objective function value, but in the last step, moving module v_λ to the slot of v_1, may not be good in reducing cost.

To address these problems, we revise the λ-exchange procedure as follows. Suppose v_1 is the first module to be moved. We compute its ϵ-neighbors and randomly pick one module, say v_2, among these modules. Then for v_2, we compute its ϵ-neighbors, and randomly pick one module, and continue in this fashion until we have λ modules. For the λ modules, we try all of their placement permutations (the total number is $\lambda!$) and exchange modules according to the least cost permutation. For example, suppose we pick modules A, D, and K. All six permutations will be tried: no exchange, $A \leftrightarrow D$, $A \leftrightarrow K$, $D \leftrightarrow K$, $A \rightarrow D \rightarrow K \rightarrow A$, $A \rightarrow K \rightarrow D \rightarrow A$. The number of solutions we search still goes exponentially with λ, but not with ϵ.

The benefit of randomly selecting ϵ-neighbors of the optimal slot is that it supports multiple passes across the placement region. Experimental results show that unidirectional circulation form algorithm quickly gets stuck at a local minimum, while permutation form algorithm has a higher probability of finding better solutions.

2.4 Problem Formulation

The problem we concerned about is described as follows. Let $M = \{m_1, m_2, ..., m_n\}$ be a set of n rectangular modules. Each module $m_i \in M$ is associated with a two tuple (h_i, w_i), where h_i and w_i denote the width and height of m_i, respectively. The area A_i of m_i is given by $h_i w_i$. Let $N = \{n_1, n_2, ..., n_k\}$ be a set of k net. Each net $n_i \in N$ is a set of modules which are connected together, like $\{m_{i1}, m_{i2}, ...\} \in n_i$. A placement (floorplan) $P = \{(x_i, y_i) \mid m_i \in M\}$ is an assignment of rectangular modules m_i's with the coordinates of their bottomleft corners being assigned to (x_i, y_i)'s so that no two modules overlap. The objective of placement/floorplanning is to minimize a specified cost metric such as a combination of the area A_{tot} and wirelength W_{tot} induced by the assignment of m_i's, where A_{tot} is measured by the final enclosing rectangle of P and W_{tot} is the summation of half the bounding box of pins for each net.

There were already many works that manipulated multilevel or hierarchical approach to disentangle the large scale issue in VLSI years ago. For example, in graph/circuit partitioning such as Chaco[13], hMetis[14], and ML[15]; in placement such as MPL[12]; in routing such as MRS[16], MR[17], and MARS[18]; in floorplanning, there was MB*-tree[10] which extended from B*-tree[1]. Because of the simplicity and identity, we choose B*-tree for easily representing the non-slicing placement and quickly computing the half-perimeter wirelength of nets.

Therefore, we decide to keep the multilevel hierarchy and the B*-tree representation of MB*-tree, but replace its simulated annealing refinement method by ϵ-neighborhood and λ-exchange algorithm for better performance. Because this algorithm combines the MB*-tree and ϵ-neighborhood and λ-exchange methods, we called our approach MBNE algorithm.

Chapter 3

The MBNE Algorithm

In this chapter, we present our MBNE algorithm for multilevel large-scale building module floorplanning/placement. This algorithm adopts a two-stage approach, clustering followed by declustering, by using the B*-tree representation. Figure 3.1 shows the MBNE algorithm flow.

The clustering operation results in two types of modules, namely primitive modules and cluster modules. A primitive module m is a module given as an input (i.e., $m \in M$) while a cluster one is created by grouping two or more primitive modules. Each cluster module is created by a clustering scheme $\{m_i, m_j\}$, where m_i (m_j) denotes a primitive or a cluster module.

In the following subsections, we give a detailed review on clustering and declustering algorithms in MB*-tree[10] and our refinement approaches in declustering phase to improve the packing results.

3.1 The Clustering Phase

In this stage, we iteratively group a set of (primitive or cluster) modules until a single cluster is formed (or until the number of cluster modules is smaller than a threshold) based on a cost metric of area and connectivity. The clustering metric is defined by the two criteria: area utilization (dead space) and the connectivity

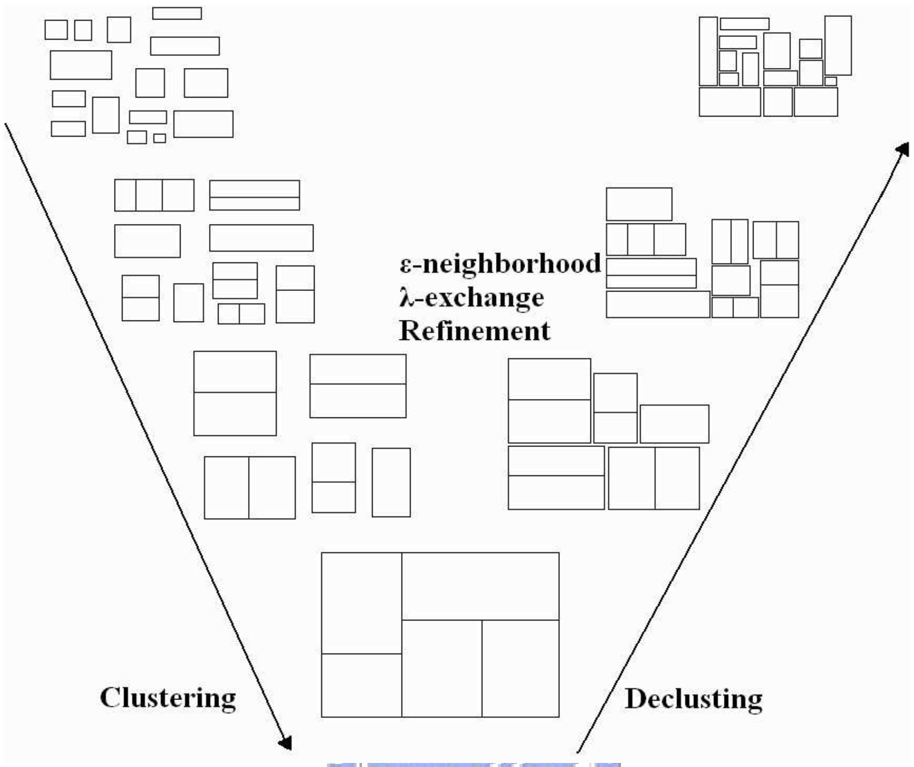

Figure 3.1: The MBNE algorithm flow. Clustering followed by declustering and using our refinement approaches in declustering phase to improve the packing results.

density among modules.

- Dead space: The area utilization for clustering two modules m_i and m_j can be measured by the resulting dead space s_{ij}, representing the unused area after clustering m_i and m_j. Let s_{tot} denote the dead space in the final floorplan P. We have $s_{tot} = A_{tot}$ - $\sum_{m_i \in M} A_i$, where A_i denotes the area of module m_i and A_{tot} the area of the final enclosing rectangle of P. Since $\sum_{m_i \in M} A_i$ is a constant, minimizing A_{tot} is equivalent to minimizing the dead space s_{tot}.

- Connectivity density: Let the connectivity c_{ij} denote the number of nets between two modules m_i and m_j . The connectivity density d_{ij} between two (primitive or cluster) modules m_i and m_j is given by

$$d_{ij} = c_{ij}/(n_i + n_j) \tag{3.1}$$

where n_i (n_j) denotes the number of primitive modules in m_i (m_j). Often a bigger cluster implies a larger number of connections. The connectivity density considers not only the connectivity but also the sizes of clusters between two modules to avoid possible biases.

Obviously, the cost function of dead space is for area optimization while that of connectivity density is for timing and wiring area optimization. Therefore, the metric for clustering two (primitive or cluster) modules m_i and m_j, $\phi :\ \{m_i,m_j\}\rightarrow\Re^{+}\bigcup\{0\}$, is then given by

$$\phi(\{m_i, m_j\}) = \alpha\hat{s}_{ij} + \frac{\beta K}{\hat{d}_{ij}} \tag{3.2}$$

where $\hat{s}_{ij}$ and $K/\hat{d}_{ij}$ are respective normalized costs for s_{ij} and K/d_{ij}, α, β and K are user-specified parameters/constants.

Based on ϕ, we cluster a set of modules into one at each iteration by applying the aforementioned methods until a single cluster containing all primitive modules is formed or the number of modules is smaller than a given threshold (and thus can be easily handled by the classical program). During clustering, we record how two modules m_i and m_j are clustered into a new cluster module m_k. If m_i is placed left to (below) m_j , then m_i is horizontally (vertically) related to m_j , denoted by $m_i\rightarrow(\uparrow)m_j$. If $m_i\rightarrow(\uparrow)m_j$, then n_j is the left (right) child of n_i in its corresponding B*-tree.(See Figure 3.2.) The relation for each pair of modules in a cluster is established and recorded in the corresponding B*-subtree during clustering. It will be used for determining how to expand a node into a corresponding B*-subtree during declustering.

3.2 The Declustering Phase

We first introduce the metric for refining floorplan/placement solutions. The declustering metric is defined by the two criteria: area utilization (dead space) and the

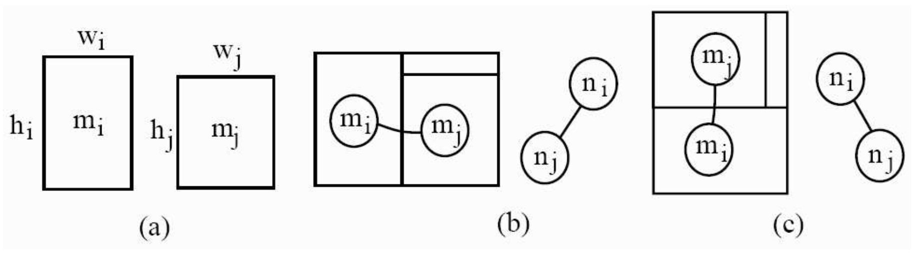

Figure 3.2: The relation of two modules and their clustering.[10] (a) Two candidate modules m_i and m_j. (b) The clustering and the corresponding B*-subtree for the case where m_i is horizontally related to m_j. (c) The clustering and the corresponding B*-subtree for the case where m_i is vertically related to m_j.

wirelength among modules.

- Dead space: Same as that defined in Section 3.1.
- Wire length: The wirelength of a net is measured by half the bounding box of all the pins of the net, or by the length of the center-to-center interconnections between the modules if no pin positions are specified. The wirelength for clustering two modules m_i and m_j , w_{ij}, is measured by the total wirelength interconnecting the two modules. The total wirelength in the final floorplan P, w_{tot}, is the summation of the length of the wires interconnecting all modules.

Obviously, the cost function of dead space is for area optimization while that of wirelength is for timing and wiring area optimization. Therefore, the metric for refining a floorplan solution during declustering, ψ_{ij}:$\{m_i,m_j\}\rightarrow\Re^+\bigcup\{0\}$, is then given by

$$\psi_{ij} = \gamma\hat{s}_{ij} + \delta\hat{w}_{ij} \tag{3.3}$$

where $\hat{s}_{ij}$ and $\hat{w}_{ij}$ are respective normalized costs for s_{ij} and w_{ij}, and γ and δ are user-specified parameters.

The declustering stage iteratively ungroups a set of previously clustered modules (i.e., expand a node into a subtree according to the B*-tree constructed at the clustering stage) and then refines the floorplan solution based on the ϵ-neighborhood and λ-exchange method.

Figure 3.3 shows the algorithm for declustering a cluster module m_k into two modules m_i and m_j that are clustered into m_k at the clustering stage. Without loss of generality, we make m_i right to or below m_j . In Algorithm Declustering (see Figure 3.3), parent(n_i), right(n_i), and left(n_i) denote the parent, the right child, and the left child of node n_i in a B*-tree, respectively. Line 1 updates the parent of n_k as that of n_i. Lines 2-5 make n_i a left (right) child if n_k is a left (right) child. Lines 6-13 deal with the case where m_i is horizontally related to m_j. If $m_i \rightarrow m_j$, then n_j is the left child of n_i and thus we update the corresponding links in Line 7. Lines 8-10 (11-13) update the links associated the right (left) child of n_k. Similarly, lines 14-23 cope with the case where m_i is vertically related to m_j.

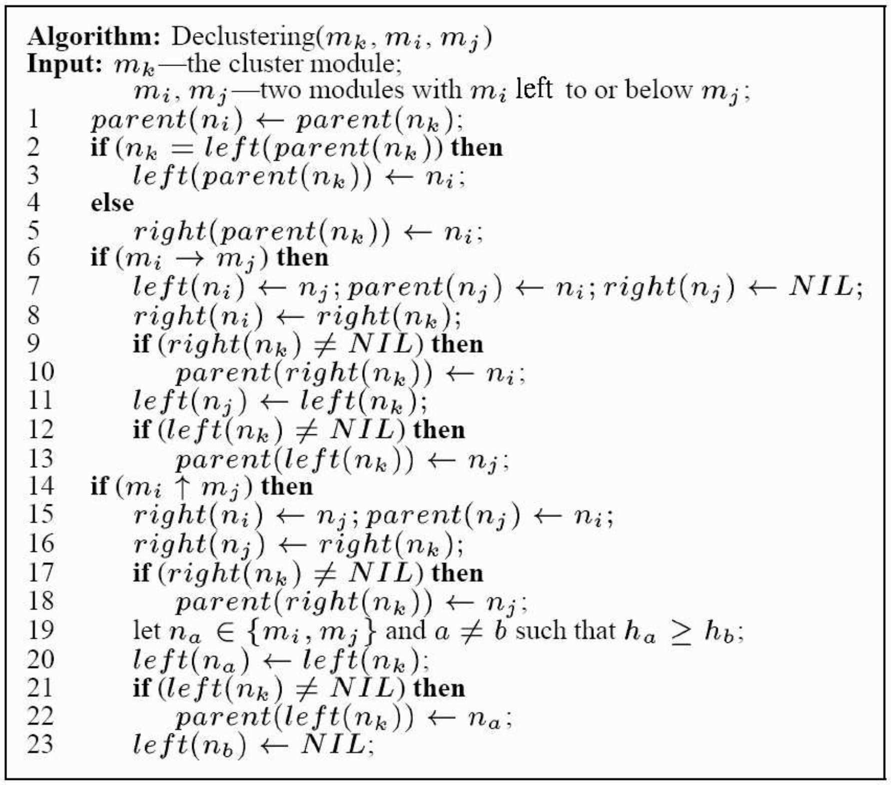

```
Algorithm: Declustering($m_k, m_i, m_j$)
Input: $m_k$—the cluster module;
       $m_i, m_j$—two modules with $m_i$ left to or below $m_j$;
1   $parent(n_i) \leftarrow parent(n_k)$;
2   if ($n_k = left(parent(n_k))$) then
3       $left(parent(n_k)) \leftarrow n_i$;
4   else
5       $right(parent(n_k)) \leftarrow n_i$;
6   if ($m_i \rightarrow m_j$) then
7       $left(n_i) \leftarrow n_j; parent(n_j) \leftarrow n_i; right(n_j) \leftarrow NIL$;
8       $right(n_i) \leftarrow right(n_k)$;
9       if ($right(n_k) \neq NIL$) then
10          $parent(right(n_k)) \leftarrow n_i$;
11      $left(n_j) \leftarrow left(n_k)$;
12      if ($left(n_k) \neq NIL$) then
13          $parent(left(n_k)) \leftarrow n_j$;
14  if ($m_i \uparrow m_j$) then
15      $right(n_i) \leftarrow n_j; parent(n_j) \leftarrow n_i$;
16      $right(n_j) \leftarrow right(n_k)$;
17      if ($right(n_k) \neq NIL$) then
18          $parent(right(n_k)) \leftarrow n_j$;
19      let $n_a \in \{m_i, m_j\}$ and $a \neq b$ such that $h_a \geq h_b$;
20      $left(n_a) \leftarrow left(n_k)$;
21      if ($left(n_k) \neq NIL$) then
22          $parent(left(n_k)) \leftarrow n_a$;
23      $left(n_b) \leftarrow NIL$;
```

Figure 3.3: The declustering algorithm.[10]

3.3 Our Refinement Method In Declustering Phase

At all levels of declustering, we apply the ϵ-neighborhood and λ-exchange method to refine the floorplan for gaining a better solution. This algorithm is inspired by the [11][12] mentioned in Section 2.3, but these two papers are for standard cell based placement. Since we focus on the large-scale circuit placement, we redefine the ϵ and λ to adjust the B*-tree representation.

The original definition of ϵ-neighborhood of module v in [11] is the modules located in slots at row i, column j where $|i\text{-}r|+|j\text{-}c| \leqq \epsilon$ and (r,c) is the optimal slot location of v. But in the non-slicing placement of large-scale circuit, the optimal slot location is hard to compute and it will shift when perturbing the modules. Hence we redefine the ϵ-neighborhood of module v as the modules away from v within ϵ branches in B*-tree. The Figure 3.4(a) is an example of 1-neighborhood of module n_2, and Figure 3.4(b) shows 2-neighborhood of module n_2.

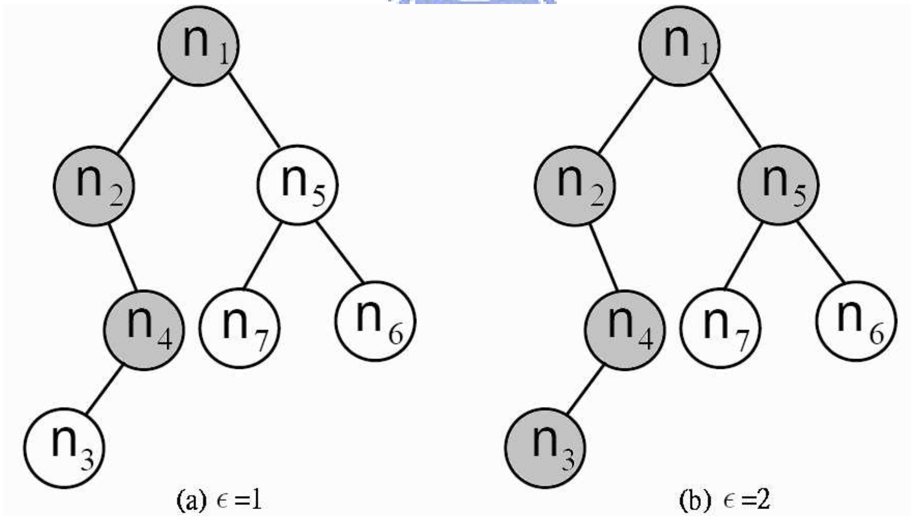

Figure 3.4: The definition of ϵ-neighborhood in our refinement method.

In our refinement algorithm, first we choose a starting module A, and select the module B which in the same net with module A. We then randomly pick the module B_λ in the ϵ-neighborhood of module B, so we have A and B_λ for 2-exchange now.

Furthermore, we can continue selecting the module C which in the same net with A and B, and randomly pick the module C_λ in ϵ-neighborhood of module C for 3-exchange. Do this sequence until we have λ modules for λ-exchange. (See Figure 3.5.)

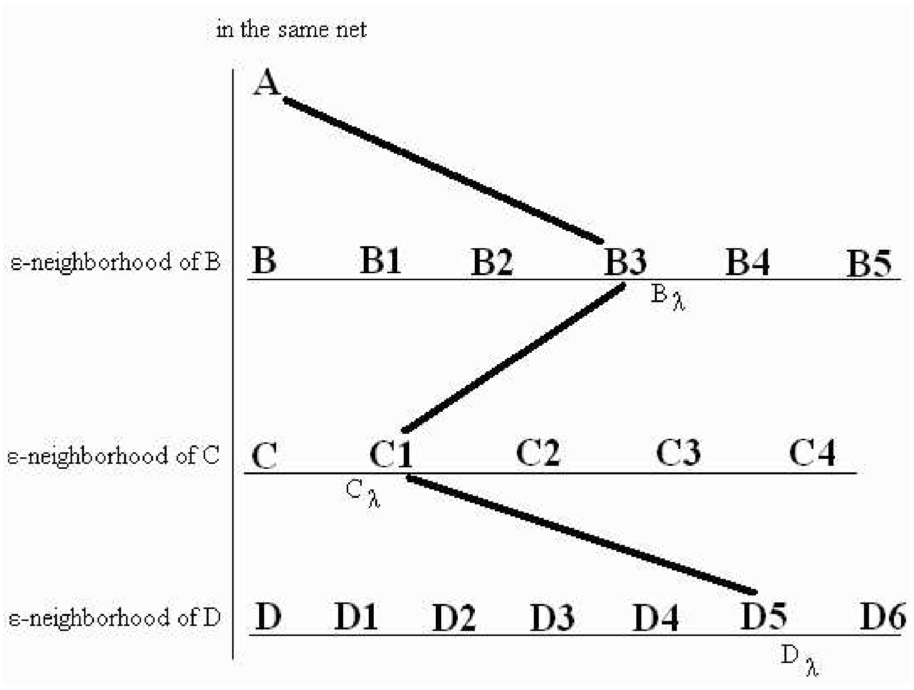

Figure 3.5: An example of λ-exchange, λ=4.

After we get all the λ modules, we try all of their placement permutations. Since this is a large-scale circuit placement, modules normally have different heights and widths. Therefore the rotation of modules will affect the placement's result. The total number of permutations is $\lambda! \times 2^\lambda$. Finally, we keep the permutation with the lowest cost and start the next turn of refinement.

3.3.1 Null Module Insertion For Further Movement

The ϵ-neighborhood and λ-exchange refinement can rotate and/or swap the modules to perturb the placement, but it can not move a module to another place. Thus, we replace one of the λ-exchange modules by null module for permutations. The null module does not connect to any module, and its height and width are equal to zero. When we decide to use null module by some probability, we insert it to be the replaced λ-exchange module's child. When a module swap with the null module, it is equivalent moving the module to be the replaced module's child. Figure 3.6 is an example of null module insertion for refinement.

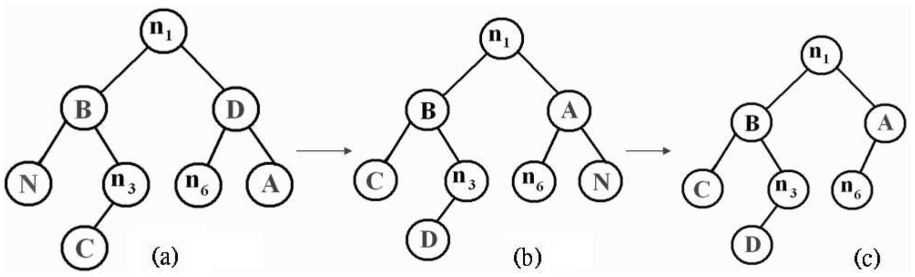

Figure 3.6: An example of null module insertion for refinement. (a)Insert modele N to replace modele B for swaping. (b)After swap, $A \to D \to C \to N \to A$. (c)Delete module N.

We have applied the null module in the ϵ-neighborhood and λ-exchange refinement, so we can combine the following three operations to perturb the placement into the lowest cost one.

- Op1: Rotate a module.
- Op2: Move a module to another place.
- Op3: Swap two modules.

3.4 Floorplanner Flow

The MBNE algorithm integrates the aforementioned three algorithms. We first perform clustering to reduce the problem size level by level and then enter the declustering stage. In the declustering stage, we perform floorplanning for the modules at each level using the ϵ-neighborhood and λ-exchange algorithm for refinement.

Figure 3.7 illustrates an execution of the MBNE algorithm. For explanation, we cluster three modules each time in Figure 3.7. Figure 3.7(a) lists seven modules to be packed, m_i's, 1≤i≤7. Figure 3.7(b)-(d) illustrates the execution of the clustering algorithm. Figure 3.7(b) shows the resulting configuration after clustering m_5, m_6, and m_7 into a new cluster module m_8 (i.e., the clustering scheme of m_8 is $\{\{m_5,m_6\},m_7\}$). Similarly, we cluster m_1,m_2, and m_4 into m_9 by using the clustering scheme $\{\{m_2, m_4\}, m_1\}$. Finally, we cluster m_3,m_8, and m_9 into m_{10} by using the clustering scheme $\{\{m_3, m_8\}, m_9\}$. The clustering stage is done, and the declustering stage begins, in which ϵ-neighborhood and λ-exchange method are applied to refine the coarse floorplan. In Figure 3.7(e), we first decluster m_{10} into m_3, m_8, and m_9 (i.e., expand the node n_{10} into the B*-subtree illustrated in Figure 3.7(e)). We then move m_8 to the top of m_9 (perform Op2 for m_8) during ϵ-neighborhood and λ-exchange refinement (see Figure 3.7(f)). As shown in Figure 3.7(g), we further decluster m_9 into m_1, m_2, and m_4, and then rotate m_2 and move m_3 on top of m_2 (perform Op1 on m_2 and Op2 on m_3), resulting in the configuration shown in Figure 3.7(h). Finally, we decluster m_8 shown in Figure 3.7(i) to m_5, m_6, and m_7, and move m_4 to the right of m_3 (perform Op2 for m_4), which results in placement with good quality shown in Figure 3.7(j).

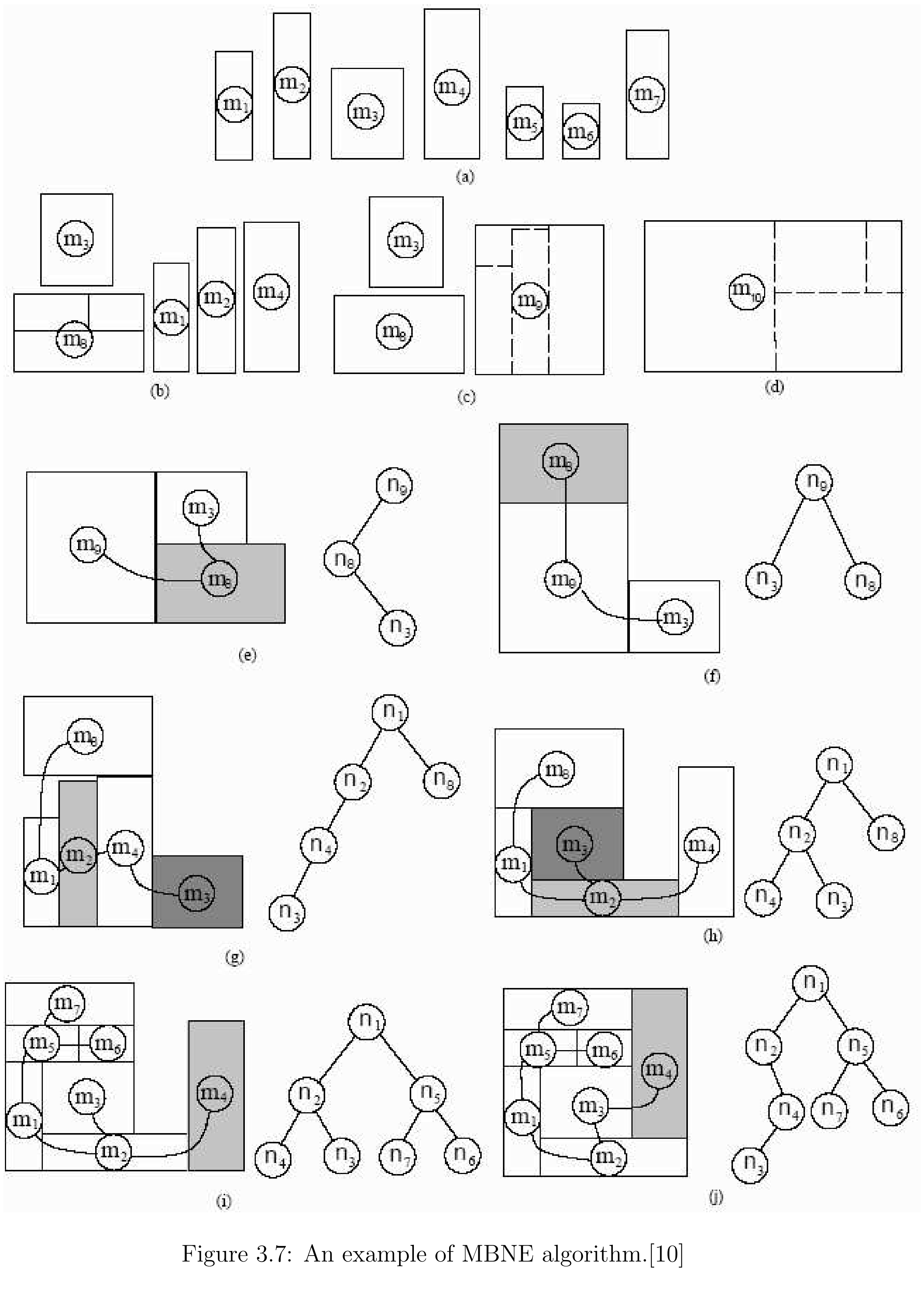

Figure 3.7: An example of MBNE algorithm.[10]

Chapter 4

Experimental Results

We implement the MBNE algorithm in C++ programming language. The platform is Intel Pentium 4 2.4GHz CPU with 1.5GB memory. We make the comparisons with the MB*-tree algorithm on benchmarks including *industry*[10], MCNC[19] and GSRC[20] suites for area, wirelength and simultaneous area and wirelength optimizations.

4.1 *Industry* with MB*-tree (Area, Wirelength, Area/Wirelength)

The circuit *industry* is a 0.18μm, 1GHz industrial design with 189 modules, 20 million gates and 9,777 center-to-center interconnections. It is a large chip design and consists of three modules with aspect ratios greater than 19 and as large as 36. In each entry of the table, we list the best/average values obtained in ten runs of MBNE and MB*-tree.

Table 4.1 shows the results of MBNE compared with MB*-tree. For area optimization, MBNE can obtain a dead space of only 1.99% while MB*-tree results in a dead space of 2.32%. For wirelength optimization, MBNE can obtain a total wirelength of only 53723 mm while MB*-tree requires a total wirelength of 55971 mm. For simultaneous area and wirelength optimization, MBNE can obtain a dead space of 9.95% and wirelength of 63583 mm while MB*-tree requires 14.45% and 67179 mm.

Package	Area optimization			Wirelength optimization	
	Area (mm^2)	Dead space (%)	Time (min)	Wirelength (mm)	Time (min)
MBNE	671.32/674.57	1.99/2.45	4.00/3.47	53723/58585	150.28/150.18
MB*-tree	673.60/679.41	2.32/3.15	3.95/3.84	55971/59759	180.45/184.54

Package	Simultaneous area and wirelength optimization			
	Area (mm^2)	Dead space (%)	Wirelength (mm)	Time (min)
MBNE	730.70/742.07	9.95/11.30	63583/63956	150.12/150.10
MB*-tree	769.10/797.28	14.45/17.37	67179/66407	153.96/159.19

Table 4.1: Comparisons for area optimization alone, wirelength optimization alone, and simultaneous area and wirelength optimization between MBNE and MB*-tree based on the circuit *industry*.

4.2 MCNC - ami49_1-200 with MB*-tree (Area)

The ami49 is the largest MCNC benchmark circuit, and we created seven synthetic circuits, named ami49_x, by duplicating the modules of ami49 by x times to test the capability of our algorithm. The largest circuit ami49_200 contains 9800 modules. Table 4.2 shows the result of MBNE compared with MB*-tree. The MBNE obtains 0.3%-1.34% improvement in dead space compared with MB*-tree for the seven ami49_x circuits.

4.3 GSRC - n100-300 with MB*-tree (Area, Wirelength)

The n100, n200, and n300 are the three GSRC benchmark circuit. We used them to compare the MBNE with MB*-tree for area and wirelength optimizations. Table 4.3 shows the number of modules, number of nets, and total area of the GSRC benchmark.

Circuit	#	Total	MB*-tree			MBNE			Improvement
	modules	area	Area	Dead space	Time	Area	Dead space	Time	in dead space
		(mm^2)	(mm^2)	(%)	(min)	(mm^2)	(%)	(min)	(%)
ami49	49	35.445	36.46	2.79	1.19	36.22	2.14	1.00	0.65
ami49_4	196	141.780	146.86	3.46	6.29	144.86	2.12	5.00	1.34
ami49_20	980	708.908	732.19	3.18	10.21	727.81	2.60	10.08	0.58
ami49_60	2940	2126.724	2211.75	3.84	16.73	2195.76	3.14	15.17	0.70
ami49_100	4900	3544.540	3704.65	4.32	20.47	3681.56	3.72	20.18	0.60
ami49_150	7350	5316.750	5590.95	4.90	26.77	5560.33	4.38	25.58	0.52
ami49_200	9800	7089.808	7478.55	5.21	31.65	7454.86	4.91	30.13	0.30

Table 4.2: Comparisons for area, dead space, and runtime between MBNE and MB*-tree with the MCNC benchmark.

Table 4.4 shows the results of MBNE compared with MB*-tree. For area optimization, MBNE can obtain dead space of only 1.64%, 2.09% and 2.08% while MB*-tree results in dead space of 2.62%, 2.39% and 2.20%. For wirelength optimization, MBNE can obtain total wirelength of only 110.982 mm, 241.696 mm and 388.162 mm while MB*-tree requires total wirelength of 111.819 mm, 244.233 mm and 391.651 mm.

4.4 Efficiency with MB*-tree

We choose four circuits from the *industry*, MCNC, and GSRC benchmark to compare for efficiency between MBNE and MB*-tree algorithm. We set the runtime of MBNE equal to 70% runtime of MB*-tree algorithm for four circuits. Table 4.5 shows the results of area, dead space and runtime of MBNE and MB*-tree. MBNE obtains dead space of 2.34%, 2.11%, 2.89% and 2.32% while MB*-tree requires dead space of 2.32%, 2.62%, 3.18% and 3.84% in these four circuits.

Circuit	# of modules	# of nets	Total area ($0.001mm^2$)
n100	100	885	179.50
n200	200	1585	175.70
n300	300	1893	273.17

Table 4.3: The number of modules, number of nets, and total area of the GSRC benchmark.

n100	Area optimization			Wirelength optimization	
	Area ($0.001mm^2$)	Dead space (%)	Time (min)	Wirelength (mm)	Time (min)
MBNE	182.490	1.64	5.00	110.982	10.03
MB*-tree	184.338	2.62	5.17	111.819	10.89
n200	Area optimization			Wirelength optimization	
	Area ($0.001mm^2$)	Dead space (%)	Time (min)	Wirelength (mm)	Time (min)
MBNE	179.452	2.09	7.00	241.696	15.37
MB*-tree	180.000	2.39	7.78	244.233	15.94
n300	Area optimization			Wirelength optimization	
	Area ($0.001mm^2$)	Dead space (%)	Time (min)	Wirelength (mm)	Time (min)
MBNE	278.964	2.08	10.01	388.162	20.40
MB*-tree	279.310	2.20	10.17	391.651	21.45

Table 4.4: Comparisons for area and wirelength optimization between MBNE and MB*-tree with the GSRC benchmark.

Circuit	# modules	Total area ($0.001mm^2$)	MB*-tree			MBNE			Improvement in time (%)
			Area ($0.001mm^2$)	Dead space (%)	Time (min)	Area ($0.001mm^2$)	Dead space (%)	Time (min)	
industry	189	657,984	673,600	2.32	3.95	673,731	2.34	2.77	29.9
n100	100	179.500	184.338	2.62	5.17	183.365	2.11	3.61	30.2
ami49_20	980	708,908	732,190	3.18	10.21	729,982	2.89	7.57	25.9
ami49_60	2940	2,126,724	2,211,750	3.84	16.73	2,199,793	3.32	11.73	29.9

Table 4.5: Comparisons for efficiency between MBNE and MB*-tree with four benchmark.

Chapter 5

Conclusion and Future Works

In this thesis, we have shown the approaches on the multilevel hierarchical floorplan/placement for large-scale circuits. With the MBNE algorithm, we can choose to optimize area only, wirelength only, or simultaneous area and wirelength with any ratio of the placement. Our MBNE algorithm combines the B*-tree representation and multilevel framework of MB*-tree, and the improved format of ϵ-neighborhood and λ-exchange refinement method. Experimental results have shown that the MBNE algorithm has better performance compared with the MB*-tree, state of the art floorplanner, in several benchmarks.

For future improvement of our placement method, developing the locally perturbation of later declutering level may solve the scalability of increased number of modules. Or we can adopt the ϵ-neighborhood and λ-exchange refinement method to another framework of algorithm, this may improve its performance.

Acknowledgement

We thank Mr. Hsun-Cheng Lee and Prof. Yao-Wen Chang for their MB*-tree platform and *industry* benchmark.

Bibliography

[1] Y.-C. Chang, Y.-W. Chang, G.-M. Wu, and S.-W. Wu. “B*-trees: A new representation for non-slicing floorplans”. In *Proceedings IEEE/ACM Design Automation Conference*, pages 458–463, 2000.

[2] P.-N. Guo, C.-K. Cheng, and T. Yoshimura. “An O-tree representation of non-slicing floorplan and its applications”. In *Proceedings IEEE/ACM Design Automation Conference*, pages 268–273, 1999.

[3] J.-M. Lin and Y.-W. Chang. “TCG: A transitive closuer graph based representation for non-slicing floorplans”. In *Proceedings IEEE/ACM Design Automation Conference*, pages 764–769, 2001.

[4] J.-M. Lin and Y.-W. Chang. “TCG-S:Orthogonal coupling of P*-admissible representations for general floorplans”. In *Proceedings IEEE/ACM Design Automation Conference*, pages 842–847, 2002.

[5] J.-M. Lin, Y.-W. Chang, and S.-P. Lin. “Corner sequence: A P-admissible floorplan representation with a worst-case linear-time packing scheme”. *IEEE Transactions on Very Large Scale Integration (VLSI) Systems*, 11(4):679–686, August 2003.

[6] H. Murata, K. Fujiyoshi, S. Nakatake, and Y. Kajitani. “Rectangle-packing based module placement”. In *Proceedings IEEE/ACM International Conference on Computer-Aided Design*, pages 472–479, 1995.

[7] S. Nakatake, K. Fujiyoshi, H. Murata, and Y. Kajitani. "Module placement on BSG-structure and IC layout applications". In *Proceedings IEEE/ACM International Conference on Computer-Aided Design*, pages 484–491, 1996.

[8] R. H. J. M. Otten. "Automatic floorplan design". In *Proceedings IEEE/ACM Design Automation Conference*, pages 261–267, 1982.

[9] D. F. Wong and C. L. Liu. "A new algorithm for floorplan design". In *Proceedings IEEE/ACM Design Automation Conference*, pages 101–107, 1986.

[10] H.-C. Lee, Y.-W. Chang, J.-M. Hsu, and H. H. Yang. "Multilevel floorplanning/placement for large-scale modules using B*-trees". In *Proceedings IEEE/ACM Design Automation Conference*, pages 812–817, 2003.

[11] S. Goto. "An efficient algorithm for the two-dimensional placement problem in electrical circuit layout". *IEEE Transactions on Circuits and Systems*, 28(1):12–18, January 1981.

[12] T. F. Chan, J. Cong, T. Kong, and J. R. Shinnerl. "Multilevel optimization for large-scale circuit placement". In *Proceedings IEEE/ACM International Conference on Computer-Aided Design*, pages 171–176, 2000.

[13] B. Hendrickson and R. Leland. "A multilevel algorithm for partitioning graph". In *Proceedings of Supercomputing*, 1995.

[14] G. Karypis and V. Kumar. "Multilevel k-way hypergraph partitioning". In *Proceedings IEEE/ACM Design Automation Conference*, pages 343–348, 1999.

[15] C. J. Alpert, J.-H. Huang, and A. B. Kahng. "Multilevel circuit partitioning". *IEEE Transactions on Computer-Aided Design of Integrated Circuits and Systems*, 17(8):655–667, August 1998.

[16] J. Cong, J. Fang, and Y. Zhang. "Multilevel approach to full-chip gridless routing". In *Proceedings IEEE/ACM International Conference on Computer-Aided Design*, pages 396–403, 2001.

[17] S.-P. Lin and Y.-W. Chang. "A novel framework for multilevel routing considering routability and performance". In *Proceedings IEEE/ACM International Conference on Computer-Aided Design*, pages 44–50, 2002.

[18] J. Cong, M. Xie, and Y. Zhang. "An enhanced multilevel routing system". In *Proceedings IEEE/ACM International Conference on Computer-Aided Design*, pages 51–58, 2002.

[19] http://www.cse.ucsc.edu/research/surf/gsrc/mcncbench.html.

[20] http://www.cse.ucsc.edu/research/surf/gsrc/gsrcbench.html.

作者簡歷

王冠中，民國六十七年六月出生於台北市。民國九十年六月畢業於國立交通大學電子工程學系，並於同年八月入伍服役。民國九十二年九月進入國立交通大學電子研究所就讀，從事 VLSI 實體設計方面相關研究。民國九十四年六月取得碩士學位，碩士論文題目為『多層架構的鄰近單元交換方法之大型電路佈局』。